### RESEARCH ARTICLE



# Rapid production of *Plasmodium* sporozoite detection paper dipstick assays using cellulose nanocrystals: Proof-of-concept for bio-based, locally developed, point-of-care devices

## Correspondence

Diego Gomez-Maldonado and Maria S. Peresin, Sustainable Bio-based Materials Laboratory, Forest Products Development Center, Auburn University, Auburn, AL 36849, USA.

Email:

d.gomezmaldonado@northeastern.edu and soledad.peresin@auburn.edu

# Present address

Diego Gomez-Maldonado, Department of Chemical Engineering, Northeastern University, Boston, Massachusetts, USA

# Funding information

National Institute of Food and Agriculture, Grant/Award Number: 2021-67021-33996

# **Abstract**

Enhanced and rapid surveillance for diseases is critical to public health and meeting United Nations' Sustainable Development Goal for Good Health and Well-being by allowing for targeted and accelerated prevention and control response strategies. Human malaria, caused by Plasmodium spp. and transmitted by mosquitoes is no exception. Advances in sustainable materials provide an opportunity to improve fast, sustainable, and equitable testing assays. Here, naturally abundant polymers and biomaterials, such as cellulose nanocrystals (CNCs) and chitosan, were used to increase antibody density deposition on the assay detection line when compared to traditional free antibody deposition, and thus the sensitivity, of easily assembled rapid tests designed to detect Plasmodium vivax infective (sporozoite) parasites in mosquitoes, a critical indicator of malaria transmission. The immobilization of antibodies onto chitosan-coated CNCs allowed for antigen detection with a lower number of antibodies used in each test; likewise, the immobilization allowed to directly place the CNC-Ab without the traditionally needed blockers layer on the paper like bovine serum albumin (BSA). This bio-based prototype of a paper-based dipstick assay shows a promising pathway for the development of rapid disease surveillance tools using sustainable and globally available materials.

This is an open access article under the terms of the Creative Commons Attribution License, which permits use, distribution and reproduction in any medium, provided the original work is properly cited.

@ 2023 The Authors. Nano Select published by Wiley-VCH GmbH.

Nano Select 2024;5:2300093. https://doi.org/10.1002/nano.202300093

<sup>&</sup>lt;sup>1</sup>Sustainable Bio-based Materials Laboratory, Forest Products Development Center, Auburn University, Auburn, Alabama, USA

<sup>&</sup>lt;sup>2</sup>College of Forestry, Wildlife and Environment, Auburn University, Auburn, Alabama, USA

<sup>&</sup>lt;sup>3</sup>US Centers for Disease Control and Prevention, Atlanta, Georgia, USA

<sup>&</sup>lt;sup>4</sup>College of Veterinary Medicine, Auburn University, Auburn, Alabama, USA

<sup>&</sup>lt;sup>5</sup>Department of Chemical Engineering, Samuel Ginn College of Engineering, Auburn University, Auburn, Alabama, USA

#### KEYWORDS

ASSURED devices, chitosan, immobilization strategy, immuno-assay

# 1 | INTRODUCTION

Malaria is responsible for over 600,000 deaths globally annually, with most cases occurring in infants in sub-Saharan African countries.<sup>[1]</sup> Determining the presence of Plasmodium spp. sporozoites (spzs) in the salivary glands of Anopheles mosquito vectors is an important disease surveillance method and malaria transmission indicator; however, current methods such as circumsporozoite (cs) enzyme-linked immunosorbent assay (ELISA) and polymerase chain reaction (PCR) are costly, time and reagent-consuming, and require additional equipment and personnel training that may not be readily available or feasible to rapidly generate sporozoite data to inform malaria control strategies.<sup>[2]</sup> Thus, developing a sensitive, fast, easy-to-use, and cost-effective device would allow for less technical and more timely characterization of Plasmodium spp. transmission, and could be used to evaluate intervention methods and assess impact of malaria control programs to improve monitoring and control the spread of this disease.

Lateral flow assays (LFA) and dipstick assays (DSA) are rapid qualitative methods to identify the presence or absence of target antigens. [3,4] Although these types of assays can be mass-produced, disparities in test availability and needs exist, as evidenced by the recent COVID-19 pandemic. For example, the need to source commercial test kits and reagents from other countries has been cited as one of the primary issues in achieving adequate testing for infectious disease management in Africa.<sup>[5]</sup> Rapid diagnostics, such as LFAs and DSAs are generally thought of as having a low cost. However, for Plasmodium sporozoite detection in mosquitoes the materials and reagents may not all be locally available and assembling the LFAs and DSAs requires multiple steps that must be performed in industrial settings. [6,7,8] These issues increase the cost and limit accessibility. In addition, the sensitivity and specificity of these assembled devices depends partly on the concentration density of antibodies and control antigens immobilized in the test line.<sup>[9]</sup> When compared to gold standard laboratory assays, such as csELISA, current rapid assays are less sensitive and accurate and need higher concentrations of the antigen in the samples tested. [3,10]

The use of naturally abundant, low-cost materials to locally develop LFAs and DSAs could increase equity in the availability of rapid testing tools for malaria transmission and control monitoring. Here, we evaluate bio-based

materials chemistry approaches using cellulose nanocrystals (CNCs) and chitosan (Ch) to determine whether rapid testing tools, such as LFAs and DSAs for Plasmodium sporozoite testing, can be developed locally using a higher density of antibodies in the test line than existing dipstick assays, for improved detection of sporozoites, using recombinant Plasmodium sporozoite positive controls. The use of globally available plant and animal product derived biobased materials may enable local LFA device fabrication which does not require costly laboratory equipment and avoids the use of large quantities of laboratory reagents, such as bovine serum albumin (BSA) blocking layers, thereby reducing the number of steps for assembly and sample processing, as well as reducing turnaround time to results. Moreover, as these are naturally occurring materials, their use will also benefit in the transition to more sustainable practices, aligning with the UN Sustainable Development Goals. This proof-of-concept study may open a path to locally developed rapid testing devices for infectious disease monitoring and management.

# 2 | EXPERIMENTAL SECTION

# 2.1 | Materials

Whatman 41 filter paper (Little Chalfont, Buckinghamshire, UK) was used as a model paper substrate to reduce interference by paper additives that are present in commercial printing papers. Sulfated cellulose nanocrystals with sodium counterions (CNC, 11.46 wt% and 1.1 wt% sulfur content) were procured from The University of Maine, however, this material can be produced from any lignocellulosic source or by bacterial fermentation.[11] Tween-20 was purchased from VWR (Randor, PA, USA). BSA and ethanolamine were purchased from Sigma-Aldrich (Burlington, MA, USA). Chitosan (65%-99% deacetylation) was procured from Alfa Aesar (Ward Hill, MA, USA). Gold nanoparticles (GNP, citric acid stabilized, 40 nm) were procured from nanoComposix (San Diego, CA, USA). Plasmodium vivax VK247 (Pv-247) antigen and capture antibodies were obtained from SeraCare (Milford, MA, USA). [12] Phosphate buffered saliner (PBS, pH 7.4) was generated in the laboratory utilizing sodium phosphate dibasic from Sigma Aldrich (Burlington, MA, USA), sodium chloride and potassium chloride (VWR, Randor, PA, USA), and potassium phosphate monobasic

(Fisher Scientific, Pittsburgh, PE, USA). Glacial acetic acid (99.9%) was purchased from Fisher Scientific (Pittsburgh, PE, USA). 1-Ethyl-3-[3-dimethylaminopropyl] carbodiimide hydrochloride (EDC) was bought from Chem-Impex International (Wood Dale, IL, USA), while Nhydroxysuccinimide (NHS) was obtained from TCI America (Portland, OR, USA). All water used in this project was ultrapure water (18.2 m $\Omega$ ) from a ThermoScientific Barnstead Nanopure unless otherwise specified.

#### **METHODS** 3

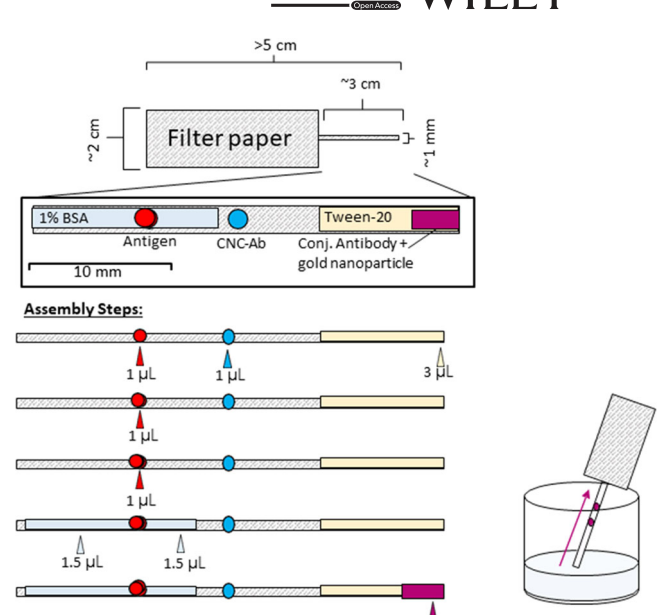
#### 3.1 Antibody ink (bio-ink) generation

The CNC mass for a 0.2% solution was calculated and separated by centrifugation for 45 minutes at 11,200 rcf. The pellet was resuspended in a 0.2% chitosan solution in 1% acetic acid. The mixture was tip sonicated for 5 minutes continuously in a 50 mL beaker with 20 KW and 20% amplitude with a Vibra Cell sonicator (Sonics & Materials, Inc Newtown, CA, USA). Then, the solution was left stirring with a magnetic stir plate overnight. A CNC-Ch pellet was formed again by centrifuging the solution at 11,200 rcf for 30 minutes.

5 μg of the *Plasmodium vivax VK247* (Pv-247) antibody (Ab) was diluted in 15 mL of PBS, then 5 µL of EDC (50 mmol) was added followed by 5 µL of NHS (200 mmol). This solution was added to the CNC-Ch pellet and redispersed with vortex mixing until the pellet broke. After 12 hours of mixing, the reaction was stopped by adding 24.4 µL of ethanolamine. The solution was then centrifuged at 2050 rcf for 1 hour and the supernatant was removed, and pellet resuspended in 300 µL of ultrapure water for characterization or 300 uL of PBS for use in the detection device. The samples were stored at -18°C until use.

#### 3.2 Characterization techniques

Hydrodynamic diameter and zeta potential changes were monitored with dynamic light scattering (DLS) in a Litesizer 500 (Anton Paar, Graz, Austria) in aqueous solutions at 0.1 wt% and pH 7.4. The reaction scheme was followed by Fourier transform infrared spectroscopy (FT-IR) with attenuated total reflectance (ATR) on freeze-dried powders with a Perkin Elmer Spotlight 400 FT-IR Imagining System with diamond/ZnSe (MA, USA) using 64 scans and a 4 cm<sup>-1</sup> resolution. For image acquisition, 180 μL of > 0.1 wt% solutions of the materials were spin coated onto silicon wafers  $(2 \times 2 \text{ cm}^2)$ . Atomic force microscopy (AFM) images were obtained using an Anton Paar Tosca



Schematic of device assembly and use.

400 in tapping mode using ARROW-NCR-20 silicon SPMsensor cantilever with a resonance frequency of 285 kHz and constant force of 42 N m<sup>-1</sup> (NanoWorld, Neuchâtel, Switzerland); the images were processed using Gwyddion software 2.49 (SourceForge).

# 3.3 | Gold nanoparticle-antibody conjugation (GNP-Ab)

The conjugation steps were performed according to the nanoComposix, Bioready protocol. Briefly, 12.5 µL of PBS buffer pH 7-9 was mixed with 40 µL of Pv-247 antibody (Ab), and 250 µL of GNP. After stability testing in a 10% NaCl solution, 25 μL of blocking buffer (with BSA) was added and mixed on a rotator for 30 minutes. Excess BSA was removed by centrifugation for 3 minutes at 3600 rcf and the resulting pellet was resuspended in 200 µL of the prepared buffer.

#### 3.4 Device assembly and testing

Filter paper was cut to the sizes shown in Figure 1 and 1 μL of Tween-20 surfactant (in PBS) was added to the right edge. 1 µL drops of the bio-ink and 3 µL of the antigen were pipetted ~25 mm from the surfactant to the bio-ink and with 5 mm between each component. In preliminary tests, as positive control 1 µL of Pv-247 antigen was deposited 3x with 1 minute resting time between each deposition and before being surrounded with 1.5 µL of BSA acting as blocking buffer. The assembly was allowed to dry at

ambient conditions for 5-10 minutes, before adding 3 µL of the GNP-Ab over the surfactant. The paper device's function was then tested by immersing it into a PBS antigen solution (10 µL in 10 mL of PBS) and left to run until the PBS reached the upper part of the device. This testing volume was selected only based on having enough amount for all sticks tested here but volume could be decreased as needed. At least four repetitions were done for the tested ink and free antibody (control) with and without BSA (Figure S1). The signal intensity comparison was done using ImageJ processing. For this, the picture was transformed to an 8-bit black and white image and color intensity was increased using a triangle threshold. Intensity was calculated with circles of 1020 pixels and ANOVA with Tukey pairwise comparison was performed on Minitab 17 statistical software (v.17.1.0.0).

# 4 | RESULTS AND DISCUSSION

# **4.1** | Antibody immobilization onto CNC-Ch

Chitosan and cellulose are known to irreversibly adsorb onto each other due to their similarity in structure. [13] This interaction is mostly driven by entropy and is consolidated by the formation of intermolecular hydrogen bonding independently of the surface charge of the cellulose or chitosan. [14,15] Thus, using this mechanism adds functionality to the CNCs without further chemical modification or energetically demanding processes. Chitosan adsorption to the CNCs and antibody immobilization to form the bio-ink were confirmed by DLS, FTIR-ATR, and AFM (Figure 2). The FTIR spectra of the initial CNCs show the characteristic absorption bands of cellulose. [16] Spectra of CNC-Ch maintain these bands, as both cellulose and chitosan are  $\beta$ -glucans, but also showed the characteristic amide band for N-H bending at 1560 cm<sup>-1</sup> of chitosan. [17] When the spectrum of the bio-ink was obtained, there was an increase in the width of the O-H stretching related to the increase of primary alcohols in the structure, as well as some possible hydrogen bonding formation.<sup>[18]</sup> Similarly, the band at approximately 1650 cm<sup>-1</sup> increased its intensity; this is attributed to hydroxyl bending, stretching of carboxyl groups, and amide bending, which correspond to the residues present in the antibody. [19] Furthermore, a band at 854 cm<sup>-1</sup> was discernible after antibody immobilization, this band has been assigned to C-H torsion due to the amino acid residues added with the antibody. [20]

The process of antibody immobilization on CNC-Ch also increased the hydrodynamic radius of the CNCs. When the chitosan was adsorbed on the surface, the particles more than doubled their size, and the zeta potential changed

from  $-10.4 \pm 2.7$  mV to  $65.9 \pm 0.97$  mV which indicated colloidal stability. Immobilization of the antibody on CNC-Ch via NHS-EDC chemistry resulted in a three-order of magnitude increase in the measured size, implying network formation and well as agglomeration consistent with the decrease in zeta potential to 15.9 + 0.56 mV (Raw plots available in Figure S2). These phenomena were also seen in the AFM images, where the CNC tended to form agglomerates and fill the PEI-coated sensor, as expected for these types of materials. [21] CNC-Ch on the other hand was seen in more isolated particles on the surface, with higher particle size, which was expected due to the higher colloidal stability and similar charges to the anchoring polymer. For the bio-ink, not many particles were present on the AFM images, as the particles were too aggregated and were not adsorbing to the wafers. Further optimization of the NHS-EDC reaction time could help to lower the network formation and avoid the loss of aspect ratio once that the antibody is presented. However, as the reaction occurred with nanometric CNC-Ch, and DLS approximates shapes to spheres, it can be expected that the agglomerate formed have irregular shapes with porosity. This porosity can still generate available surfaces for the interaction of the gold-proved antibodies and antigens to the bio-ink.

# **4.2** Assay assembly and antigen detection

Figure 3 shows results following dipstick experiments with Pv-247 antigen conjugated with gold nanoparticles. Preliminary assays (not shown) were performed with Pv-247 antibody diluted in PBS-only and diluted in the BSA containing blocked buffer, but no clear detection signal could be observed. As shown in Figure 3 all the assay strips using the bioink had a visible signal with only 1 µL of sample. In addition, results could be obtained without the use of an extra layer such as the BSA used in the controls. Furthermore, only 16.7 ng of antibody were needed for each test, which is lower than the 100-ug required for each well in csELISA<sup>[22]</sup> and an improvement compared to the commercial dipstick assays for sporozoite detection. [10] The test showed high sensitivity as the saturation of the ink dot can be observed with a black color in the test strip when a 5 ng mL<sup>-1</sup> antigen-PBS solution was used. Statistical analysis of contrasted repetitions was done for the different systems using the CNC-Ab and the free antibody with and without BSA (Figure S3). The ANOVA results demonstrated no statistical difference when the BSA was used with the CNC-Ab. However, a 4-fold higher greater contrast was obtained with the CNC-Ab compared to the BSA immobilized Ab. The results obtained with free antibody and no BSA were statistically the same as the

	Hydrodynamic radius [μm]	Zeta potential [mV]
CNC	$0.20 \pm 0.03$	$-10.4 \pm 2.87$
CNC-Ch	$0.53 \pm 0.05$	$65.9 \pm 0.97$
CNC-Ab	$344 \pm 65.5$	$15.9 \pm 0.56$

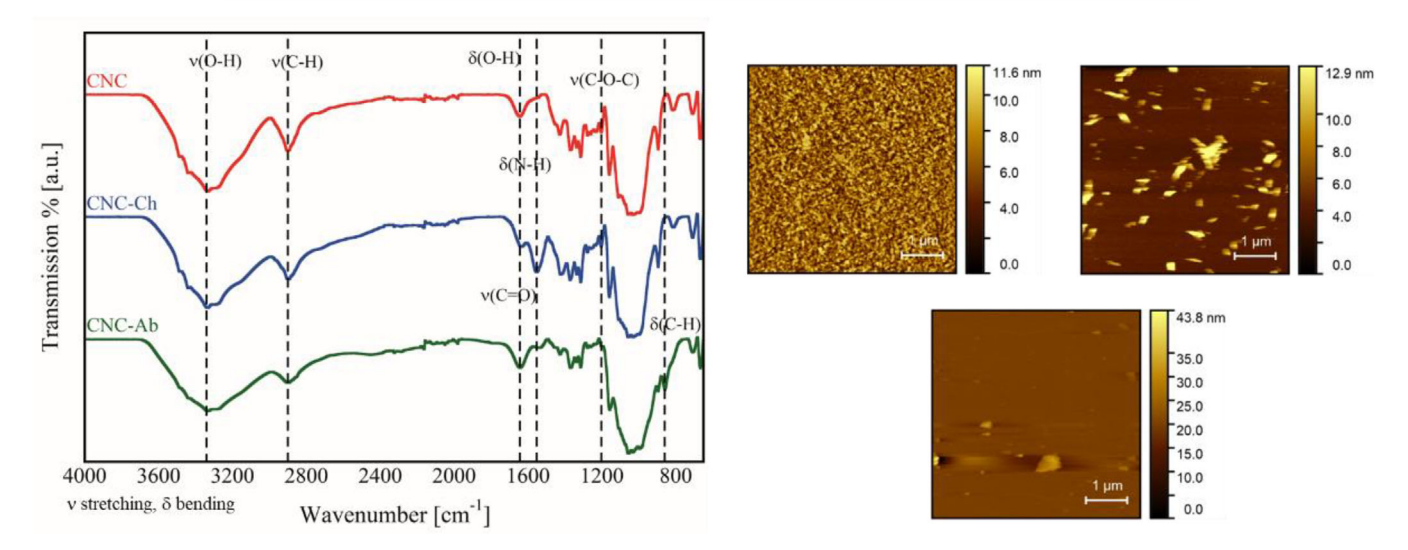


FIGURE 2 Results of the characterization of the CNCs, CNC-Ch, and CNC-Ab. (top) shows a table containing the hydrodynamic radius and zeta potential obtained from DLS measurements, (left) the FTIR-ATR spectra following the chemical modification, and (right) show the AFM images for CNC, CNC-Ch, and CNC-Ab with a  $5 \times 5 \,\mu m$ . CNCs, cellulose nanocrystals; CNC-Ch, chitosan modified cellulose nanocrystals; CNC-Ab, antibody loaded cellulose nanocrystals.

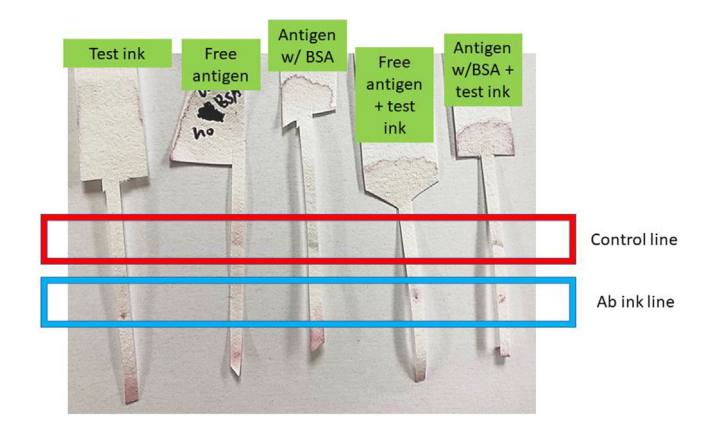


FIGURE 3 Results of the test ran with free antigen, delimited with BSA or not, and using the bio-ink or free antibody in the detection line. The first device only had the bio-ink, the second and third were used for the control line setting without and with blocking BSA; the fourth device has a control line without BSA and the bio-ink, while the last device has a BSA blocked control line and the bio-ink. BSA, bovine serum albumin.

untreated paper, showing the significant improvement of this immobilization strategy for point-of-care diagnostics.

The devices shown in Figure 3 were assembled in approximately 10 minutes without the use of specialized equipment or the need for specialized training. This

makes them advantageous for point-of-care devices in low-resource regions. Similarly, the reactants used (bio-ink, antigen, surfactant, and GNP-Ab) do not need extra processing or cold-chain storage and could be distributed easily, aligning with United Nations Sustainable Development Goal number 3 "Good Health and Well-being". The devices also provided a presence or absence response in less than 10 minutes, ideal for rapid detection. [23,24]

This methodology can also be adapted for the immobilization of the other protein antigens on LFA or DSAs, to decrease volume requirements of constituent reagents, avoid use of BSA or other blocking solutions in the flow pathway as shown here in the bio-ink line, and potentially increase sensitivity. The small volume required might also allow for the generation of multiplex assays<sup>[23,25]</sup> where this dot can be added to the substrate next to each other, decreasing unwanted mixtures. Likewise, the use of CNC-Ch as a base platform for antibody immobilization, versus the direct immobilization of antibody onto the substrate (e.g., nitrocellulose), brings this work closer to LFAs that can be produced by simple methods such as inkjet printing or direct writing. [26,27] These methods are being considered as the new targets for POC applications as they can be easily adapted to laboratories worldwide without high-cost equipment.



To transition to these target methods, bio-ink viscosity can be readily adjusted for use with different printers or in microfluidic devices by including other bio-based materials<sup>[27]</sup> or by altering the concentration of CNC-Ab used in the inks.<sup>[28]</sup> Demonstrating that CNC-Ch can be used to enhance detection methods provides a foundation for the use of CNC in more sensitive quantitative devices, as well as upcoming technologies such as cantilever bear arrays produced from CNC.<sup>[29]</sup>

# 5 | CONCLUSIONS

This research showed that globally available, sustainable bio-based materials are promising for producing a simple, rapid test for *Plasmodium vivax* VK247 antigen using CNC-Ch-bound antibodies. Immobilization of the antibodies on CNC-Ch enabled simple detection without the use of additional blocking steps. This proof-of-concept, using a well-established assay for infective malaria parasite detection in mosquitoes, highlights the potential for the use of renewable materials, which are widely available. This approach is promising for meeting the World Health Organization Guidelines for simple and local development of ASSURED (Affordable, Sensitive, Specific, User-friendly, Rapid/Robust, Equipment-free and Deliverable) point-of-care diagnostics. [23]

# **AUTHOR CONTRIBUTIONS**

Diego Gomez-Maldonado; Conceptualization; Methodology; Investigation; Analysis; Visualization; Writing – original draft. Gabriel Au; Methodology; Investigation; Visualization. Sarah Zohdy; Conceptualization; Resources; Writing. Virginia A. Davis; Conceptualization; Resources; Writing. Maria S. Peresin; Conceptualization; Resources; Supervision; Writing.

# **ACKNOWLEDGMENTS**

The authors want to thank BEI Resources and the Malaria Research and Reference Reagent and Resource Center (MR4) for providing the *Plasmodium vivax* 247 sporozoite ELISA Reagent Kits. Similarly, the authors want to thank Dr. Alice C. Sutcliffe for her input and help during the writing and clearance process for this work. The authors acknowledge USDA NIFA 2021-67021-33996 for funding. The authors would like to acknowledge the Northeastern University Snell Library for covering the full APC of this article and their effort to make research accessible for everyone.

# CONFLICT OF INTEREST STATEMENT

The authors declare no conflict of interest in this work. The findings and conclusions in this report are those of the author(s) and do not necessarily represent the official position of the Centers for Disease Control and Prevention.

# DATA AVAILABILITY STATEMENT

The data that support the findings of this study are available from the corresponding author upon reasonable request.

# ORCID

Diego Gomez-Maldonado https://orcid.org/0000-0003-4199-4091

Gabriel Au https://orcid.org/0000-0003-4093-7925
Sarah Zohdy https://orcid.org/0000-0001-5316-0567
Virginia A. Davis https://orcid.org/0000-0003-3126-3893
Maria S. Peresin https://orcid.org/0000-0003-2619-5320

# REFERENCES

- 1. J. Wambani, P. Okoth, J. Trop. Med 2022, 2022, 7324281.
- H. Noedl, K. Yingyuen, A. Laoboonchai, M. Fukuda, J. Sirichaisinthop, R. S. Miller, Am J Trop Med Hyg 2006, 75, 1205.
- M. A. Appawu, K. M. Bosompem, S. Dadzie, U. S. McKakpo, I. Anim-Baidoo, E. Dykstra, D. E. Szumlas, W. O. Rogers, K. Koram, D. J. Fryauff, *Trop. Med. Int. Health* 2003, 8, 1012.
- S. Kasetsirikul, M. J. A. Shiddiky, N. T. Nguyen, Microfluid Nanofluid 2020, 24, 1.
- E. K. Oladipo, A. F. Ajayi, A. N. Odeyemi, O. E. Akindiya, E. T. Adebayo, A. S. Oguntomi, M. P. Oyewole, E. M. Jimah, A. A. Oladipo, O. E. Ariyo, B. B. Oladipo, J. K. Oloke, *Drug Discov Ther* 2020, 14, 153.
- C. Christian, A. Bo, S. Schabel, M. Biesalski, Microfluid Nanofluidics 2014, 16, 789.
- J. Kim, X. E. Cao, J. L. Finkelstein, W. B. Cárdenas, D. Erickson, S. Mehta, Malar J 2019a, 18, 313.
- M. Sajid, A. N. Kawde, M. Daud, J. Saudi Chem. Soc. 2015, 19, 689.
- 9. Y. Deng, H. Jiang, X. Li, X. Lv, Microchim Acta 2021, 188, 379.
- J. R. Ryan, K. Dave, E. Emmerich, L. Garcia, L. Yi, R. E. Coleman, J. Sattabongkot, R. F. Dunton, A. S. T. Chan, R. A. Wirtz, *Med Vet Entomol* 2001, *15*, 225.
- D. Gómez-Maldonado, M. Hernández-Guerrero, R. López-Simeon, I. J. Arroyo-Maya, J. Campos-Terán, In *Lignocellulosics*, pp. 91, Elsevier 2020. https://doi.org/10.1016/B978-0-12-804077-5.00004-X
- Malaria Research and Reference Reagent Resource Center (MR4), Plasmodium circumsporozoite ELISA directions. 2017. https://www.beiresources.org/Catalog/ BEIMonoclonalAntibodies/MRA-890.aspx
- 13. T. Mishima, M. Hisamatsu, W. S. York, K. Teranishi, T. Yamada, *Carbohydr Res* **1998**, *308*(3–4), 389.
- 14. D. Gomez-Maldonado, I. Filpponen, I. B. Vega Erramuspe, L. Johansson, M. F. Mori, R. J. Babu, M. N. Waters, M. S. Peresin, *Surf. Interfaces* **2022**, *33*, 102192.
- H. Orelma, I. Filpponen, L. S. Johansson, J. Laine, O. J. Rojas, Biomacromolecules 2011, 12, 4311.
- D. Klemm, B. Philipp, T. Heinze, U. Heinze, W. Wagenknecht, In Methods, First ed, Wiley-VCH, 1998.

- 17. P. Kumar Dutta, J. Dutta, V. S. Tripathi, *J Sci Ind Res* **2004**, *63*, 20.
- 18. M. Fan, D. Dai, B. Huang, Fourier Transform Materials Analysis, pp. 274, 2012. https://doi.org/10.5772/35482
- A. Saeed, G. A. Raouf, S. S. Nafee, S. A. Shaheen, Y. Al-Hadeethi, *PLoS One* 2015, 10, 1.
- 20. U. Mohan, P. Gogoi, S. K. Baruah, Orient J Chem 2016, 32, 1003.
- E. J. Foster, R. J. Moon, U. P. Agarwal, M. J. Bortner, J. Bras, S. Camarero-Espinosa, K. J. Chan, M. J. D. Clift, E. D. Cranston, S. J. Eichhorn, D. M. Fox, W. Y. Hamad, L. Heux, B. Jean, M. Korey, W. Nieh, K. J. Ong, M. S. Reid, S. Renneckar, R. Roberts, Jo Anne Shatkin, J. Simonsen, K. Stinson-Bagby, N. Wanasekaraq, J. Youngblood, *Chem Soc Rev* 2018, 47, 2609.
- 22. A. C. Sutcliffe, S. R. Irish, E. Rogier, M. Finney, S. Zohdy, E. M. Dotson, *Malar J* **2021**, *20*, 1.
- 23. J. Li, J. Macdonald, Biosens Bioelectron 2016, 83, 177.
- 24. A. K. Yetisen, M. S. Akram, C. R. Lowe, *Lab Chip* **2013**, *13*, 2210
- J. Kim, X. E. Cao, J. L. Finkelstein, W. B. Cárdenas, D. Erickson,
   S. Mehta, Malar J 2019, 18, 1.
- 26. Y. L. Han, J. Hu, G. M. Genin, T. J. Lu, F. Xu, Sci Rep 2014, 4, 1.

- 27. B. Kannan, S. Jahanshahi-Anbuhi, R. H. Pelton, Y. Li, C. D. M. Filipe, J. D. Brennan, *Anal Chem* **2015**, *87*, 9288.
- J. M. Buffa, U. Casado, V. Mucci, M. I. Aranguren, *Cellulose* 2019, 26, 2317.
- P. Saha, N. Ansari, C. L. Kitchens, W. R. Ashurst, V. A. Davis, ACS Appl Mater Interfaces 2018, 10, 24116.

# SUPPORTING INFORMATION

Additional supporting information can be found online in the Supporting Information section at the end of this article.

How to cite this article: D. Gomez-Maldonado, G. Au, S. Zohdy, V. A. Davis, M. S. Peresin, *Nano Select* **2024**, *5*, 2300093.

https://doi.org/10.1002/nano.202300093